International Journal of Chemical and Biochemical Sciences
(ISSN 2226-9614)

Journal Home page: www.iscientific.org/Journal.html

Ptychotis verticillata Duby essential oil inhibits mild steel corrosion in 1M HCl

Fatine Elfarhani[1], Moussa Ouakki[2,3*], Asmae Oubihi[4], Zakia Aribou[1], Omar Belhadj[2], Kelthoum Tarfaoui[5], Zineb Guessous[4], Bousalham Srhir[1,3], Mohammed Cherkaoui[2,3], Mohamed Ebn Touhami[1]

[1]Laboratory of Advanced Materials and Process Engineering, Faculty of Sciences, University Ibn Tofail PB. 133-14000, Kenitra, Morocco

[2]Laboratory of Organic Chemistry, catalysis and Environment, Faculty of Sciences, Ibn Tofaïl University, PO Box 133, 14000, Kenitra, Morocco.

[3]National Higher School of Chemistry (NHSC), University Ibn Tofail BP. 133-14000, Kenitra, Morocco

[4]Laboratory of Natural Resources and Sustainable Development, Department of biology, Faculty of Science, University Ibn Tofail, Kenitra, Morocco.

[5]Laboratory of Biodiversity and Natural Resources, Faculty of Sciences, Ibn Tofail University, Kenitra, Morocco

Abstract

As a way to shield the mild steel surface against the aggressive chloride ions attack from the HCl 1M medium. The ability of *Ptychotis verticillata* Duby (PVD) was investigated as a corrosion inhibitor. The uppermost compound making up the PVD essential oil is thymol. A series of experimental studies encompassing electrochemical tests, and surface analysis were limelight fascinating outcomes, revealing a very high efficiency since the addition of the PVD essential oil concentrations especially from 1g/L with 93,8 % until 2g/L to reach 96.8 % at ambient temperature 298K. From the PDP results, the inhibitor shows a mixed type behavior with a predominance of cathodic site. At high temperatures, PVD essential oil shows a slight increase in corrosion current compared to the ambient temperature, nevertheless, its inhibition efficiency remains higher. The adsorption process followed was the Langmuir adsorption isotherm, and a strong physisorption process was revealed. The composition and the surface morphology of the formed layer were confirmed by the SEM/EDX analysis.

Keywords: *Ptychotis verticillata* Duby, Corrosion, inhibition, mild steel, electrochemical, surface analysis.

Full length article **Corresponding Author*, e-mail: moussa.ouakki@uit.ac.ma

1. Introduction

Owing to the fact that corrosion is the main engineering problem in the present industry evolution in the modern age, prevention methods are the focal points for all researchers [1]. Controlling the corrosion process, especially in aggressive media was often achieved by employing inhibitors [1]. By bringing down the corrosion rate by the adsorption process. Generally, the required inhibitor should be distinguished by a set of characteristics comprehending good efficiency at very low concentrations and protect the metal surface, thermally stable and chemically inert, possess good surfactant, beat low coast, non-toxic, and available [2]. Many corrosion inhibitors are inorganic substances like phosphates, chromates, dichromates, silicates, borates, tungstates, molybdates, and arsenates, and others are organic compounds containing polar function groups, heteroatoms such as nitrogen, oxygen, and sulfur in addition to π electrons in the conjugated system.

Both present a high ability to protect and prevent metals from the corrosion process even in aggressive circumstances due to their structural properties. Nevertheless, they don't obey the last three inhibitor-required conditions above, which made the researchers look for new solutions adequate to the environment's safety [3-4]. Nowadays, the researches in the corrosion field are aligned toward green organic compounds that are characterized as available and renewable source substances that do not contain heavy metals or poisonous compounds [5]. As a magnificent alternative, plant extract has attracted all the researcher's curiosity in the green organic inhibitor's chemistry field, as being fits the required characteristics for a corrosion inhibitor, environmentally acceptable, low cost, readily available, and biodegradability, in addition to their ecological compatibility, due to their biological genesis [5-6]. The plant extracts are generally a complex natural mixture possessing a variety of molecular structures having different chemical, biological, and physical properties such as carotenoids, phenols, vitamins, and flavonoids [5]. Among the Plant extract products; there is the EO (Essential Oil), which is a very vintage term that had been used for the first time in the sixteenth century. Pursuant to AFNOR, the term refers to the "product obtained from vegetable raw material, either by distillation with water or steam, or from the pericarp of citrus fruits by a mechanical process, or by dry distillation" [7]. A diversity of aromatic plants could be the birthplace of the EO's product. From a chemical viewpoint, the EO's could contain more than 100 compounds with different concentrations, which makes them a complex nature mix. whereas just two or three major components are at higher concentrations than the others in trace amounts, appended in two chemical groups: terpenes and phenylpropanoids [5]. The EO derived from various plants is used to prepare coatings, which are used in tiny concentrations to protect the surface of metals from corrosive environments [2,8]. The thymol is among the main chemical structures in the terpenes group, which are responsible for their distinctive aromas, ketones, acids, aldehydes, esters, and alcohols. and it is the major component of Ptychotis verticillate duby, known as Nûnkha is an aromatic plant widespread in North African countries and widely used in different fields as traditional medicine as an antispasmodic, antidiabetic, and antipyretic agent, also an antiseptic for its antifungal and antibacterial properties [9]. Assiduous scrutiny of the recent publications reveals that nearly all tested EO compounds have established a good achievement as eco-friendly inhibitors against corrosion phenomena in assorted mediums. Table 1 stipulates a set of authors' investigations on the natural EO behavior as green corrosion inhibitors toward different metals and alloys in different media. In the present work, the Nunkha EO properties will be discovered in a different field, with a new manner, as a corrosion inhibitor in order to figure out the PVD Essential oil special characteristics on controlling the corrosion process and its behavior toward the protection of mild steel surface in acidic medium. To achieve the aim, a set of studies have been done such as the electrochemical studies including the potential dynamic polarization and impedance spectroscopy in different concentrations and temperatures. besides the surface analysis using the SEM and EDX analysis.

2. Conditions for the experiments

2.1. Material and medium

Electrochemical experiments were performed on mild steel specimens where the chemical composition is given in Table 2. Before each test, the specimens were polished using abrasive paper of grade 80 to 2000 in order to obtain a mirror-finish. Prior usage; the item was cleaned with distilled water, degreased with acetone, and then dried. The harsh medium (1.0M HCl) used in this study was made by diluting commercial acid with distilled water. The tested inhibitor concentration ranged from 0.5 to 2.0 g/l.

2.2. Characterization of the chemical composition of essential oil

The chemical composition of the PVD essential oil was assessed using GC-MS. The samples were examined on a Thermo Fisher gas chromatograph, which was connected to the mass spectrometry system (model GC ULTRA S/N 210729). A 5% phenyl methyl silicone HP-5 capillary column (30 m × 0.25 mm × thickness 0.25 µm) was employed for separation. The temperature was programmed from 50 ◦C and increased at a rate of 4 ◦C/min, reaching 200 ◦C after an initial 5-minute hold. Nitrogen (N_2) served as the carrier gas at a flow rate of 1.8 mL/min. The split mode was applied with a flow rate of 72.1 mL/min and a ratio of 1/50. The injector and detector temperatures were set at 250 ◦C, and the final hold time was 48 minutes. For analysis, 1 µL of essential oil was manually injected after dilution in hexane. The chemical composition of PVD essential oil obtained was manifested in Table 3.

3. Experimental

3.1. Electrochemical study

The electrochemical tests were fulfilled in a conventional three-electrode cell consisting of 1cm^2 of mild steel substrate as a working electrode, ESC as a reference electrode, and a platinum wire as a counter-electrode, connected to the Potentiostat (Radiometer Analytical PGZ 100). in 1M HCl. The mild steel substrate was plunged for close to 1800 seconds until reaching a steady potential (E_{ocp}) ahead of each electrochemical test. Potential Dynamic Polarization (PDP) curves were achieved by polarization from -900 to -100 mV/Ag with a scan rate of 1 mV s^{-1} at E_{ocp}. The inhibitory efficiency (η_{pp} %) is calculated by the following Equation (1) [24-25]:

$$\eta_{PP} = \frac{i^{0}_{corr} - i_{corr}}{i^{0}_{corr}} \times 100 \qquad (1)$$

Where i°_{corr} and i_{corr} are the values of corrosion current densities in the absence and presence of inhibitor, respectively. Electrochemical Impedance Spectroscopy (EIS) measurements were performed into a frequency range of 100 kHz to 100 mHz with a 10mV amplitude at the E_{ocp}. The corresponding percent of inhibition performance (η_{EIS}) is expressed in the following manner Equation (2)

$$\eta_{EIS} = \frac{R_{ct} - R^{0}_{ct}}{R_{ct}} \times 100 \qquad (2)$$

$$\theta = \frac{R_{ct} - R^{0}_{ct}}{R_{ct}} \qquad (3)$$

With R^0_{ct} and R_{ct} are the charge transfer resistances without and with PVD essential oil, respectively, and θ is the recovery rate.

3.2. SEM/EDX analyses

Surface morphological analyses utilizing SEM and EDX were done to support electrochemical findings. After being polished, cleaned, and dried the mild steel specimens with and without PVD essential oil were examined after immersion for 6 hours into 1.0 M HCl solution. EDX analysis and SEM investigations were conducted together.

4. Results and discussion

4.1. Electrochemical studies

4.1.1. Polarization studies

With a view to acknowledging the PVD essential oil behavior as a corrosion inhibitor in an aggressive media, the potential-dynamic polarization experiment was fulfilled. Figure 1 manifests the potential curves of the unfolded process on the mild steel surface immersed in HCl 1M aggressive solution in the dearth and presence of different concentrations of PVD essential oil. Whereas the kinetics parameters are manifested in Table 4 and illustrated as below; Corrosion Potential (E_{corr}), Corrosion current density (I_{corr}), Tafel slopes (βc and βa), and inhibition efficiency (η %). The large linearity of the cathodic curves that go along with the corrosion density decrease by increasing the PVD essential oil concentrations is divulging the corroboration of the Tafel's law in the cathodic domain, and that the lowering of hydrogen evolution is held back by pure activation kinetics [26]. In the anodic domain, by adding PVD essential oil concentrations, two linear portions were heeded. Go-ahead with the lowest polarization potentials, the anode current density vaguely increases between -0.4 and -0.3eV potential domain. Further than -0.3eV toward the positive region, once the desorption potential Ed exceeds the anodic current density increases rapidly. According to the literature a rise of corrosion current with a slow move of the corrosion potential is related to the desorption process [27]. Which means beyond the mentioned potential the inhibitors major molecules exposed to a desorption of the mild steel surface. However, the current density still lower than the Blanc. The authors speculate that the efficiency of inhibitors depends on the electrode potential [28]. The corrosion potential exhibits a significant step toward the cathodic region, connotes that the inhibitor major molecules affect the hydrogen evolution mechanism rather than the dissolution metal. The displacement of the potential corrosion by the presence of different concentrations of PVD essential oil, indicate that the primarily mechanism taking by the inhibitor is based on the energy effect and not the blocking mechanism [29]. From Table 4, The displacement of corrosion potential is about -58,-54,-36 and -15mV for 0.5, 1,1.5 and 2 g/l according to the authors this range of displacement which is superior than -85 referred to the mixed type of PVD essential oil inhibitor with predominance of cathodic region confirming the control of the hydrogen evolution rather than the metal dissolution [30]. The corrosion current present a huge decrease to reach 20 µA/cm for 2 g/L. The change in both Tafel's slopes □a and □c confirms the mixed type of the PVD essential oil inhibitor that set in on both corrosion reactions [31]. The corrosion efficiency shows a qualitative leap from 0.5 to 1 g/l about 71.2% to 94.2% until reaching the best performance at 2g/L with 97.9%. This is due to the chemical properties of the PVD essential oil components [32].

4.1.2. EIS studies

To corroborate the PDP investigation and going further to a deep understanding of the mechanism reaction of the PVD essential oil inhibitor by studying its effect on electric double layer and the dielectric properties at metal-solution interfaces with explanation of the dynamics of electrochemical reactions developing through the adsorbed film, The EIS is called. The Figure 2 present the Nyquist and Bode plots in the lack and presence of the PVD essential oil in different concentrations at 289K. First able, from the Nyquist plot, the semicircle shape in the impedance curves stipulate the capacitive behavior of the mild steel corrosion process in 1M HCl media [26,33]. The large increase of the capacitance loop is clearly shown by increasing the inhibitor concentration. indicate the adsorption behavior of the major compounds of the PVD essential oil on the mild steel surface especially on reaching big amount, as a result the formation of protective layer through the charge transfer process. after the depressed capacitance loop and the maintain of the same shape even after including the PVD essential oil at different concentrations, it can be said that the corrosion mechanism is not affected [34]. Following the Bode plots, The charge transfer process was the main responsible of the formation of the thin layer protector through the big adsorption of the major molecules of PVD essential oil inhibitor on the mild steel surface which is clearly manifested from the widening and the single maxima pics at the middle frequency [35]. However, at low frequency a huge increment of log Z and phase angle comparing to the blank (Z_{Blanc} = 36.57 Ω cm, α = 51°) outreach 1122.01 Ω cm and 70° for Z_{PVD} and phase angle respectively, which stipulate the decrease and improvement of corrosion activity process. Whereas at high frequency the log Z and phase angle tend to 0, setting down the increase of the resistance behavior around the mild steel electrode and reference electrode [34]. EIS spectra were explored by the Randle's equivalent circuit which is delineated in Figure 3. An equivalent circuit involves a solution resistor (R_s), a double-layer capacitance (C_{dl}), and a charge transfer resistor (R_{ct}). As a means to a more error-free fit of impedance data, the constant phase element (CPE) is replaced in lieu of double layer capacitance (C_{dl}), because the metal /electrolyte interface system does not act as a pure capacitor [36]. The impedance is designated by the expression below Equation (4):

$$Z_{\mathrm{CPE}} = \frac{1}{Q} \times \frac{1}{(jw)^n} \qquad (4)$$

where the "Q" is the coefficient of proportionality of the CPE, "ω" corresponds to the angular frequency and "n" as a surface homogeneity factor. The values of the double layer capacitance (C_{dl}) were computed as below in Equation (5) [26]:

$$C_{\mathrm{dl}} = \sqrt[n]{(Q \times R_{\mathrm{p}}^{1-n})} \qquad (5)$$

The EIS parameters were extracted in the Table 5, on intensifying the PVD essential oil concentrations the R_{ct} values get bigger attaining 1093 Ω cm^2 by 2 g/L. While a large decrease of C_{dl} manifests. Explained by the adsorption and quick switch between the water molecules and the major compounds of PVD essential oil on blocking the available active site on the mild steel surface, besides a decrease in the dielectric cst that enhance the adsorptive ability of the major compounds of PVD essential oil and assure a good protection [37]. The n_{dl} factor shows higher just after the adding of the PVD essential oil inhibitor, which points to the formation of an organic film on the mild steel surface that provide protection and enhance the homogeneity of the surface aspect [38]. Starting from 1g/L until 2g/L the PVD essential oil inhibitor performs highly with an efficiency of 97% for 2g/L that could interpreted by the power of the donor groups, the polar functional groups, and the π-bonds of the major molecules of PVD essential oil to interact with the iron atom d-orbitals, establishing a protective layer sheltering the metal surface.

4.2. Adsorption isotherm

Molecular adsorption is the main process carried out by the organic inhibitors as prevention method of corrosion on the metal surface to form a protective layer as went into above [39]. The adsorption mechanism of PVD essential oil was initially determined by adsorption model fitting**.**[40] To acquire an equitable adsorption isotherm for PVD essential oil on mild steel surface, several mathematical models called adsorption isotherms that appraise the adsorbate quantity (i.e., molecules/ions of inhibitors) on the absorbent (i.e., the surface of the metallic substrate) at a constant temperature are needed, including Langmuir, Temkin, Frumkin, Freundlich, Florye Huggins and Bockrise Swinkels [39]. From between the models, the best fit with the experimental data was presented by Langmuir isotherm. Which it can clearly see from the R^2 coefficient Langmuir isotherm (0.99998). This model suggests that an attraction or repulsion remains between the species absorbed on the metal surface [25]. The Langmuir plot of PVD essential oil adsorption on mild steel in an acidic medium is presented in Figure 4 and the adsorption parameters is listed in Table 6. Equation for the Langmuir isotherm is given as Equation (6):

$$C_{\text{inh}} = \left(\frac{\theta}{1-\theta}\right) \times \left(\frac{1}{K_{\text{ads}}}\right) \quad (6)$$

Where K_{ads} is the adsorption-desorption equilibrium constant [34,39]. From the Table 6, the K_{ads} parameter that refers to the adsorption powerness, present a high value stands for a good adherence of the PVD essential oil's major molecules on the mild steel [41]. Another parameter of the adsorption process, obtained from Kads, is the free energy of adsorption (ΔG◦ads) which is specified below Equation (7):

$$\Delta G^{\circ}_{\text{ads}} = -RT \text{ Ln } (1000 \times K_{\text{ads}}) \quad (7)$$

Where 1000 is the g/l concentration of water in the solution [42]. Pursuant to literature, the value of ΔG°_{ads} below 20 kJ/mol is featured to weak physisorption, whilst above 40kJ/mol is marked to strong chemisorption [43]. Howbeit, physisorption is weak only for small molecules, but it becomes much stronger for large molecules than chemisorption [34]. For PVD essential oil inhibitors the ΔG°_{ads} show a value of -20.9KJ/mole that suggest strong physisorption interactions due to the largeness of the inhibitor molecules. That confirms the inhibition efficiencies shown in the previous PDP and EIS results.

4.3. Effect of Temperature

Among the parameters influencing the corrosion rate and affect straightly the organic compounds properties is Temperature [44]. The Figure 5 presents the polarization curves for mild steel in HCl medium without and with the optimum concentration 2g/L of PVD essential oil inhibitor in different temperature. The Table 7 illustrates the polarization parameters. Initially, comparing to the blank we can clearly see that the anodic and cathodic curves decrease at different temperature and show a perfect parallelism which means that the PVD essential oil inhibitor keeps control both reactions, besides the anodic curves that appear parallel at high current density in a further anodic potential after being at low current density before -0.3 mV [45]. Which could be explain by a stability of the major molecules of PVD essential oil inhibitor on the metal surface after being adsorbed [17]. Nevertheless, comparing between different temperature, the increase of this last affect the performance of the PVD essential oil inhibitor and cause an increase in the corrosion current. The corrosion potential show little move toward the negative region, which suggest the metal dissolution enhancement [20]. From Table 7, for all temperatures the PVD essential oil shows a high efficiency, talking about 97.9%, 96.5%, 94.0% and 90.6% for 298K, 308K, 318K and 328K, respectively regardless the little diminution especial at 318 K due to the weakness of the wander wall bonds toward the temperature that cause a backed in the adsorption process of the major components of inhibitor [46]. However, the strong electrostatic interactions of the major molecules of PVD essential oil inhibitor are verified by the maintain of the good efficiency. The variety of the anodic and cathodic slops confirms the permanency of the inhibitor in controlling both corrosion reactions under the temperature effect [47].

4.4. Activation parameters of the corrosion process

The Figure 6 shows that the corrosion reaction can be regarded as an Arrhenius-type process Equation (8). The activation parameters were calculated according to Arrhenius formula and transition state Equation (9):

$$ln\, i_{\text{corr}} = \frac{-E_{\text{a}}}{R} \times \left(\frac{1}{T}\right) + ln\, A \quad (8)$$

$$ln\left(\frac{i_{\text{corr}}}{T}\right) = \left(ln\left(\frac{R}{Nh}\right) + \frac{\Delta S_{\text{a}}}{R}\right) - \left(\frac{\Delta H_{\text{a}}}{R} \times \frac{1}{T}\right) \quad (9)$$

The activation energy of metal dissolution is mentioned as E_a, A is Arrhenius pre-exponential factor, and R is the Universal Gas Constant, while T is absolute. ΔH_a is the activation enthalpy and ΔS_a is the entropy activation. The values for the slopes have been used for determining the E_a of the mild steel dissolution for both uninhibited and inhibited electrolytes and the values for activation parameters are collated in Table 8.

That shows a high value of E_a in the presence of the inhibitor reverse to its absence. Indicating the formation of a barrier energy that cause a retardation to the corrosion process on the Mild steel [23]. The rise of activation energy in presence of the inhibitor as compared to the blank is attributed to electrostatic attractiveness between metal and the inhibitor [48]. The enthalpy (ΔHa) and the entropy (ΔSa) of activation parameters were derived from the transition state formula Equation (9). The ΔHa either shows a high value with the positive sign confirm that the corrosion process underwent decrease in the presence of PVD essential oil inhibitor following an endothermic process. [49]. We should speak briefly of the major value of E_a than the enthalpy value, which indicate that the process of corrosion brings in a gas reaction, which is the hydrogen evolution [50]. While the ΔSa shows a large increase with a negative sign that could be explained by the haphazardness of corrosion site due to the desorption of water molecules that increase the solvent entropy, due to the adsorption of inhibitors molecules that decrease the metal interface entropy, which calls quasi-substitution [51].

4.5. Surface analysis

4.5.1. Scanning Electron Microscopy (SEM) Coupled by EDX

The SEM images and EDX spectra of the Mild steel after 6 hours of immersion in the presence and absence of PVD essential oil are manifested in Figure 7. In the absence of inhibitor, the surface morphology appears heterogeneous with cracks and formed oxide, that show up clearly from the EDX spectrum, in which the corrosion element such Fe, Cl and O clearly manifest with very high intense and percentage as shown in Table 9. In contrary, in the presence of PVD essential oil, the Fe peaks appear with a large decrease with suppression of Cl element while the O and C peaks are enhanced due to their presence within the chemical composition of the PVD essential oil. As a result, a smooth aspect, no cracks and uniform surface clearly appeared. Which confirms the adsorption of the PVD essential oil molecules on the mild steel surface and the protection of the surface from the aggressive attacks of chloride ions [51].

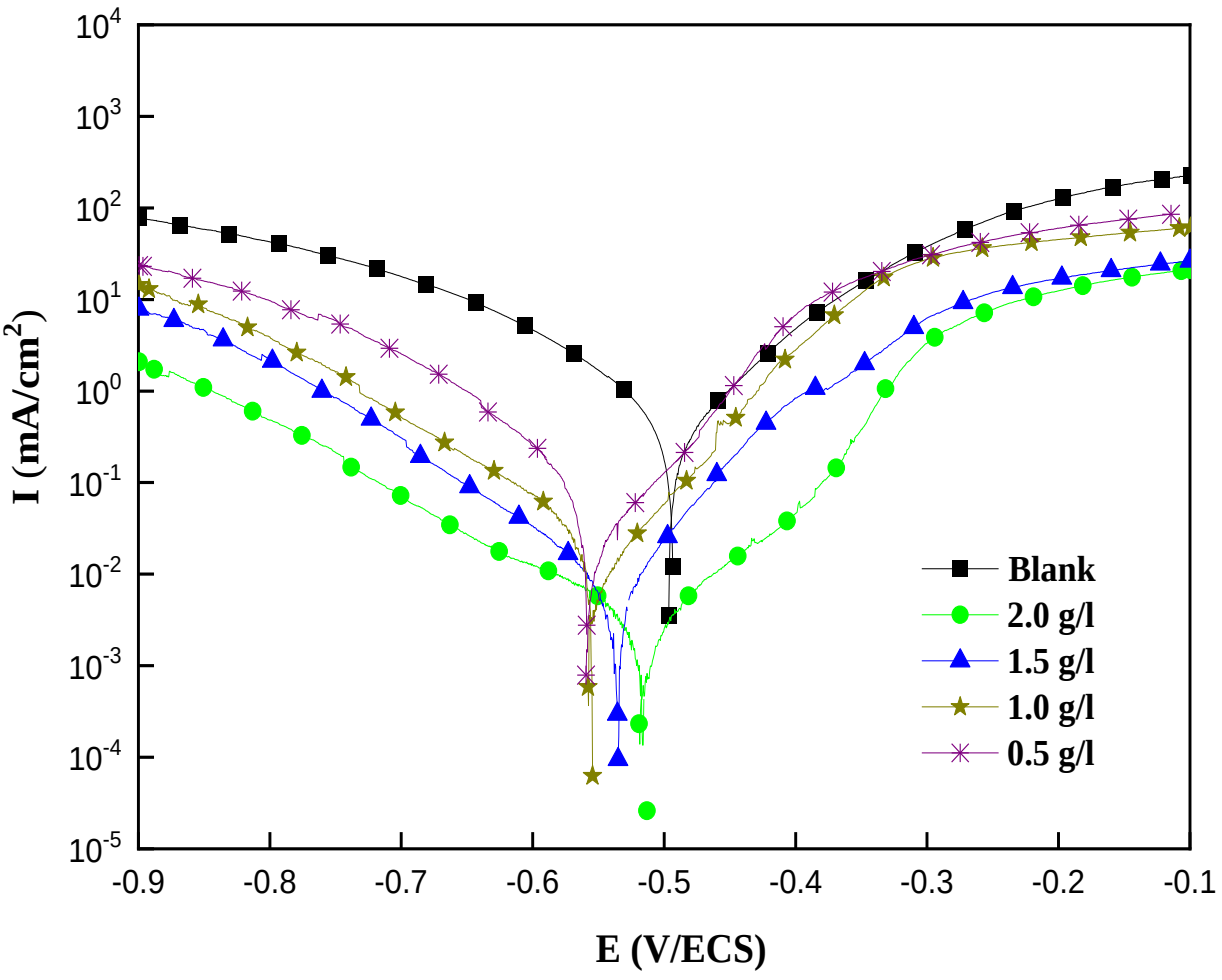

Figure 1 : Polarization curves of mild steel in the absence and presence of PVD essential oil at 298 K.

Table 1: EO used as green corrosion inhibitors for metals and alloys in various media.

Essential Oils	Metal/ Medium	Efficiency	Main Observation	Ref
Artemisia abrotanum	1M HCl / Mild steel	83.9 %	Optimum Concentration: 2 g/L Nature: Mixed inhibitor Adsorption: -	[10]
Artemisia mesatlantica	1M HCl /Carbon steel	92 %	Optimum Concentration: 3 g/L Nature: Mixed inhibitor Adsorption: Physisorption	[11]
Eucalyptus globulus	0.5M H_2SO_4 / C38 Steel	81%	Optimum Concentration: 6 g/L Nature: Mixed inhibitor Adsorption: Physisorption	[12]
Tetraclinis articulata	1M HCl / Carbon steel	80%	Optimum Concentration: 2g/L Nature: Mixed inhibitor Adsorption: Physisorption	[13]
Pistacia lentiscus	1M HCl / Mild steel	96.34 %	Optimum Concentration: 1g/L Nature: Mixed inhibitor Adsorption: Physisorption	[14]
Lavandula dentata	1M HCl / Steel	90 %	Optimum Concentration: 2 g/L Nature: cathodic inhibitor Adsorption: Chemisorption	[15]
Orange peel	1M HCl / Mild steel	94.8%	Optimum Concentration: 3 g/L Nature: Mixed inhibitor Adsorption: Physisorption	[16]
Mentha spicata	1M HCl / Steel	97 %	Optimum Concentration: 2 g/L Nature: Mixed inhibitor Adsorption: Physisorption	[17]
Thymus sahraouian	1M HCl/ Mild steel	77.82 %	Optimum Concentration: 2 g/L Nature: Mixed inhibitor Adsorption: Physisorption	[18]
Asteriscus graveolens	0.5M H_2SO_4 / Mild steel	82.89 %	Optimum Concentration: 3 g/L Nature: Mixed inhibitor Adsorption: Physisorption	[19]
Cinnamomum verum (Cinnamon)	0.5M H_2SO_4 / Copper	89.62 %	Optimum Concentration: 150 ppm Nature: cathodic inhibitor Adsorption: Physisorption	[20]
Pistacia lentiscus	0.5M H_2SO_4 / Steel	81.2 %	Optimum Concentration: 2 g/L Nature: Mixed inhibitor Adsorption: Physisorption	[21]
Salvia aucheri mesatlantica	0.5M H_2SO_4 / Steel	86.12 %	Optimum Concentration: 2 g/L Nature: Mixed inhibitor Adsorption: Chemisorption	[22]
Allium sativum	0.5M H_2SO_4 / Copper	97.4 %	Optimum Concentration: 1 g/L Nature: cathodic inhibitor Adsorption: -	[23]

Table 2: Chemical composition of mild steel (%wt).

Elements	Fe	C	Si	Mn	P	S	N	Cr	Co	Mo	Ni	Cu
% wt	Bal	0.04	0.41	1.46	0.07	0.03	0.08	18.5	0.16	0.33	7.81	0.51

Table 1: Chemical composition of *Ptychotis verticillata* duby (PVD) essential oil.

	Compound	R.Time	%
1	o-Cymene	10.589	14.87
2	D-Limonene	10.743	10.11
3	γ-Terpinène	11.612	3.34
4	L-terpinen-4-ol	15.271	2.83
5	Thymol	18.145	54.32
6	o-Thymol	18.275	13.57
7	2,5-dimethylthiophene	39.310	0.98
	Total identified %		99.99

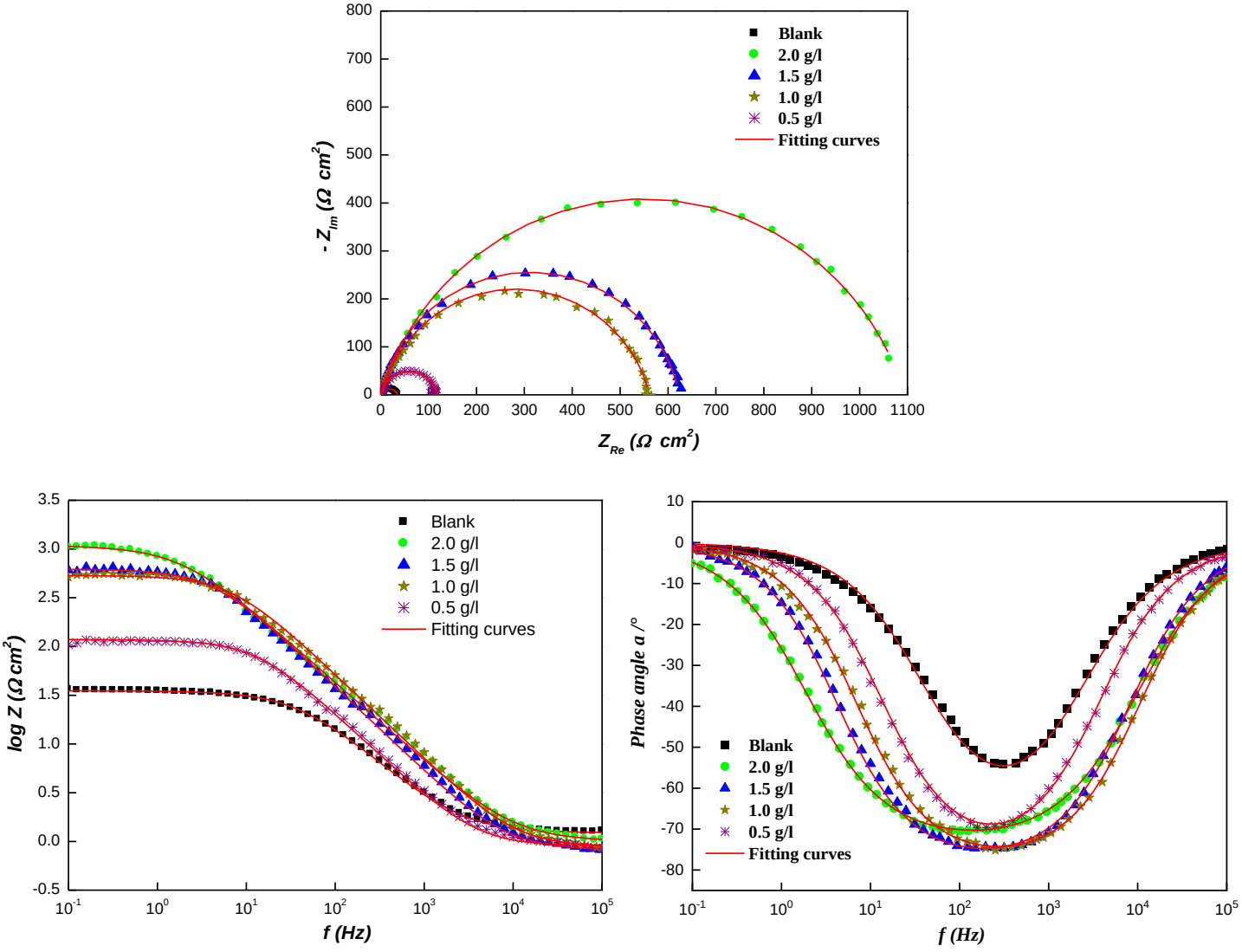

Figure 2: Nyquist (a) and Bode (b) graphs for M-Steel in the blank medium without and with PVD essential oil.

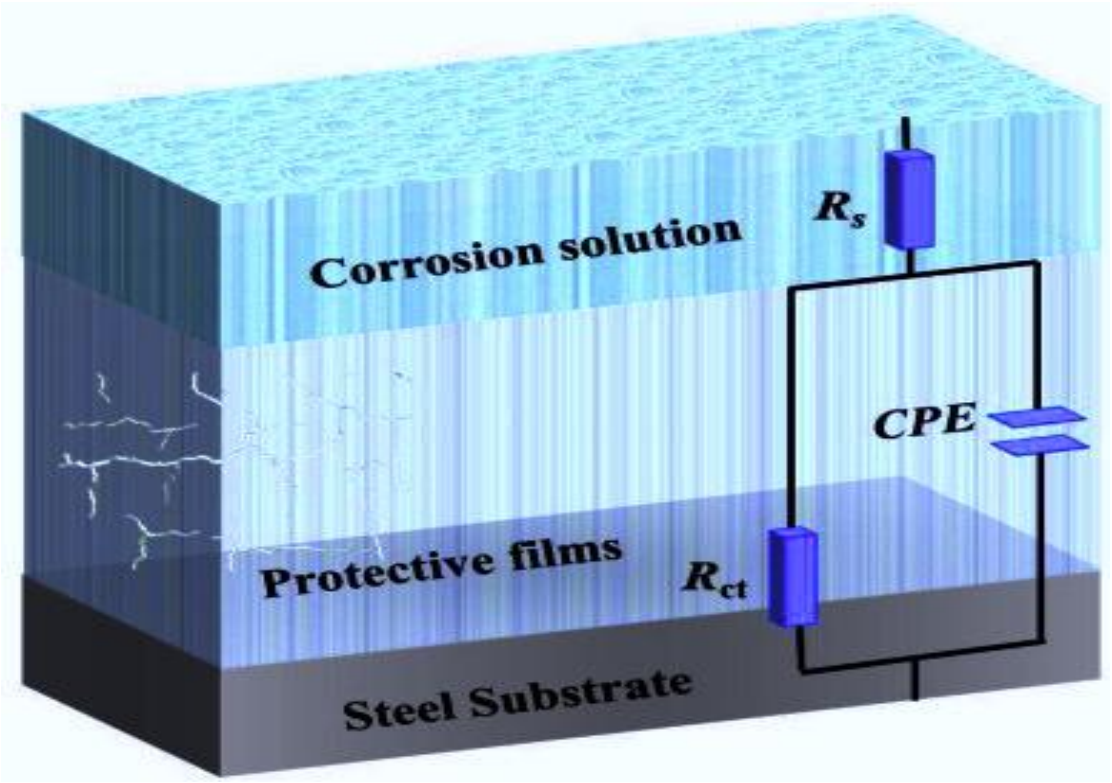

Figure 3: Electrochemical equivalent circuit used to fit the EIS data.

Table 2: Polarization parameters for M-steel corrosion in 1M HCl in the presence and absence of PVD essential oil at 298K.

Medium	Conc. g/l	$-E_{corr}$ mV/ECS	i_{corr} µA cm^{-2}	$-\beta_c$ mV dec^{-1}	β_a mV dec^{-1}	η_{PP} %
1.0 M HCl	--	498	983	140	150	-
PVD	0.5	556	283	137	144	71,2
	1.0	552	58	133	140	94,1
	1.5	534	50	131	137	94,9
	2.0	513	20	128	132	97,9

Table 3: EIS parameters for M-steel in 1 M HCl without and with inhibitors at 298 K.

	Conc. (g/l)	R_s (Ω cm^2)	R_{ct} (Ω cm^2)	C_{dl} (µF cm^{-2})	n_{dl}	Q (Ω^{-1} S^n cm^{-2})	Θ	η_{imp} %
1.0 M HCl	--	1.1	34.7	121.0	0.773	419	-	-
PVD	0.5	0.9	117	99.2	0.870	276	0.703	70,3
	1.0	1.2	559	44.3	0.850	177	0.938	93,8
	1.5	0.8	623	34.8	0.875	152	0.944	94,4
	2.0	0.9	1093	29.5	0.817	120	0.968	96,8

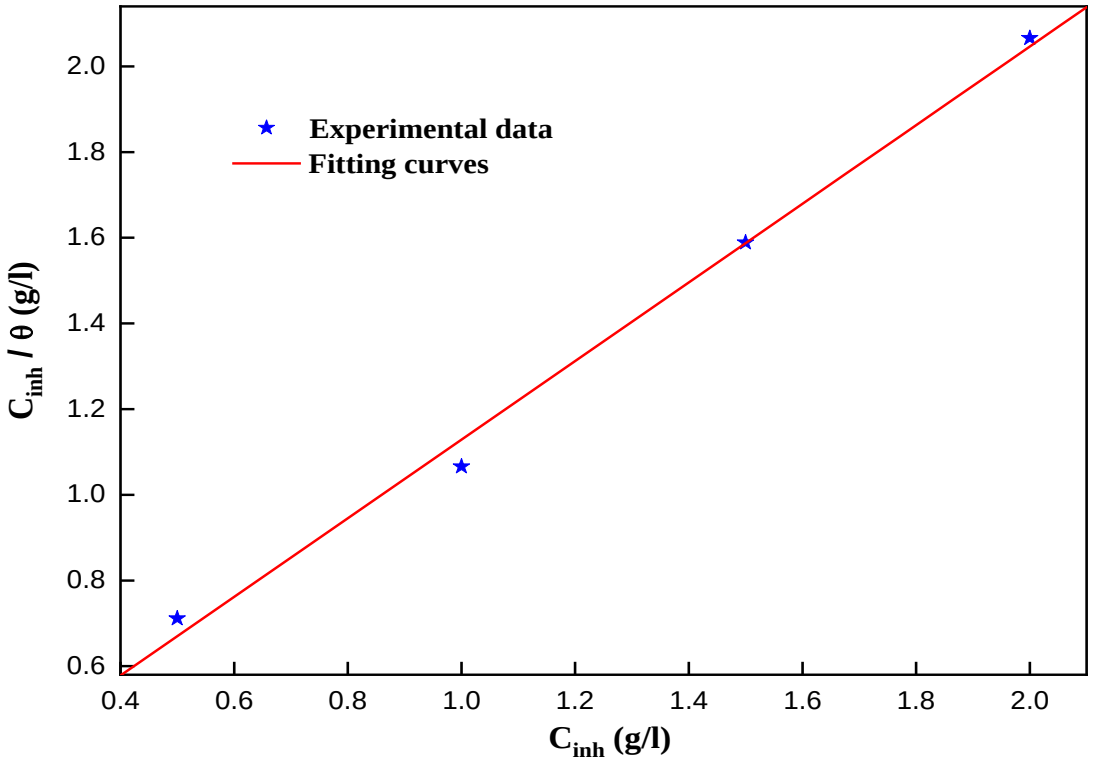

Figure 4: PVD essential oil Langmuir adsorption isotherm plots at 298 K on the mild steel surface.

Table 4: Thermodynamic parameters for the adsorption of PVD essential oil on M-steel in 1 M HCl at 298 K temperature.

Inhibitor	K_{ads} (L/g)	ΔG_{ads} (KJ/mol)	R^2	Slope
PVD	4.73	-20.9	0.99715	0.92

Table 5: Polarization parameters for mild steel corrosion in 1M HCl in the presence and absence of PVD at different temperature.

Medium	Tempe K	$-E_{corr}$ mV/ECS	i_{corr} µA cm^{-2}	$-\beta_c$ mV dec^{-1}	βa mV dec^{-1}	η_{PP} %
Blank	298	498	983	140	150	-
	308	477	1200	184	112	-
	318	487	1450	171	124	-
	328	493	2200	161	118	-
PVD	298	513	20	128	132	97,9
	308	515	42	165	111	96,5
	318	542	87	151	122	94,0
	328	531	206	157	116	90,6

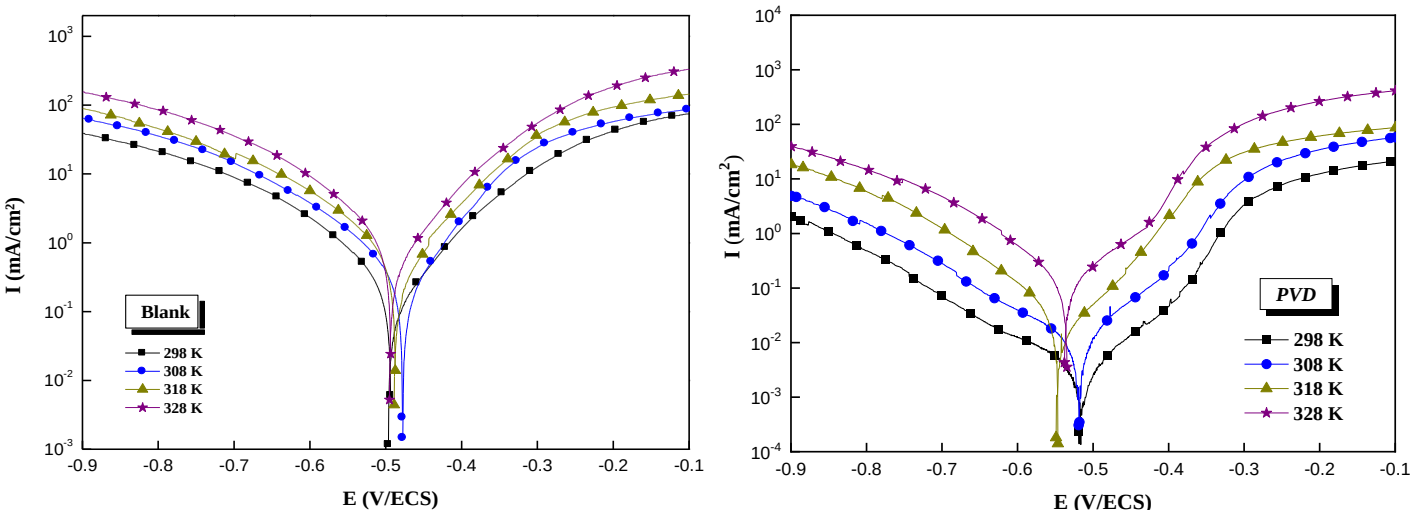

Figure 5: Polarization curves for mild steel without and with 2g/L of PVD essential oil at different temperatures.

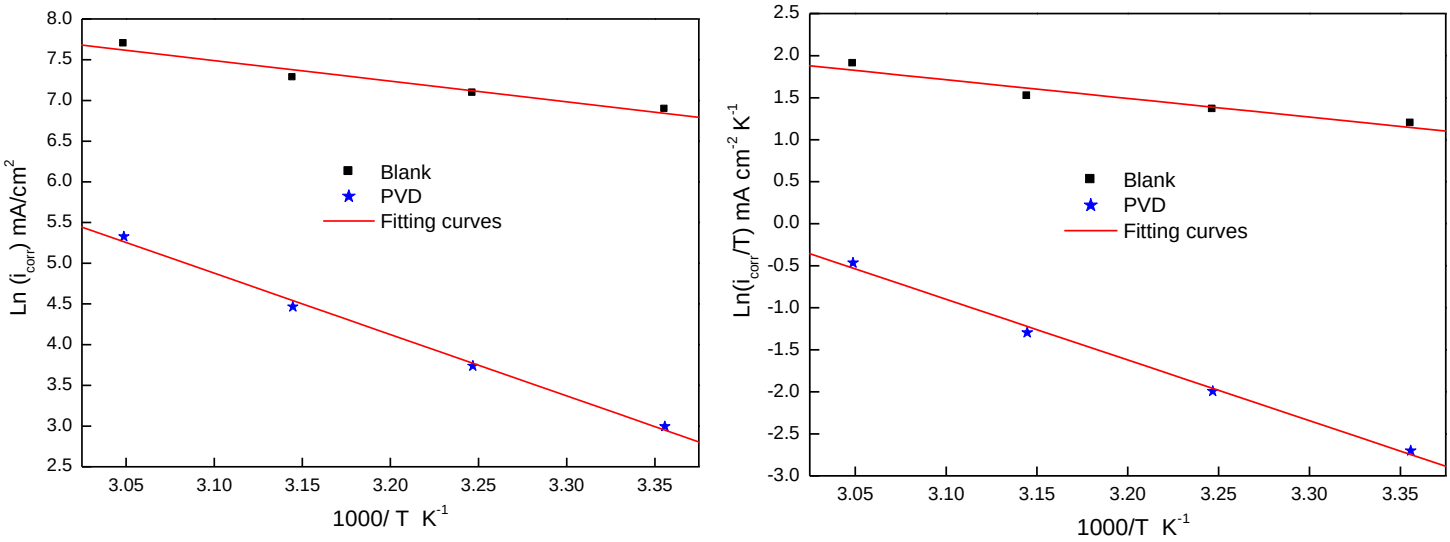

Figure 6: Arrhenius plots of mild steel in HCl medium without and with PVD essential oil at different temperatures.

Table 6: Activation parameters of PVD oil essential.

Medium	Ea (KJ/mol)	ΔHa (KJ/mol)	ΔSa (J/mol.K)
Blank	21.0	18.5	-126.0
PVD	62.7	60.1	-18.8

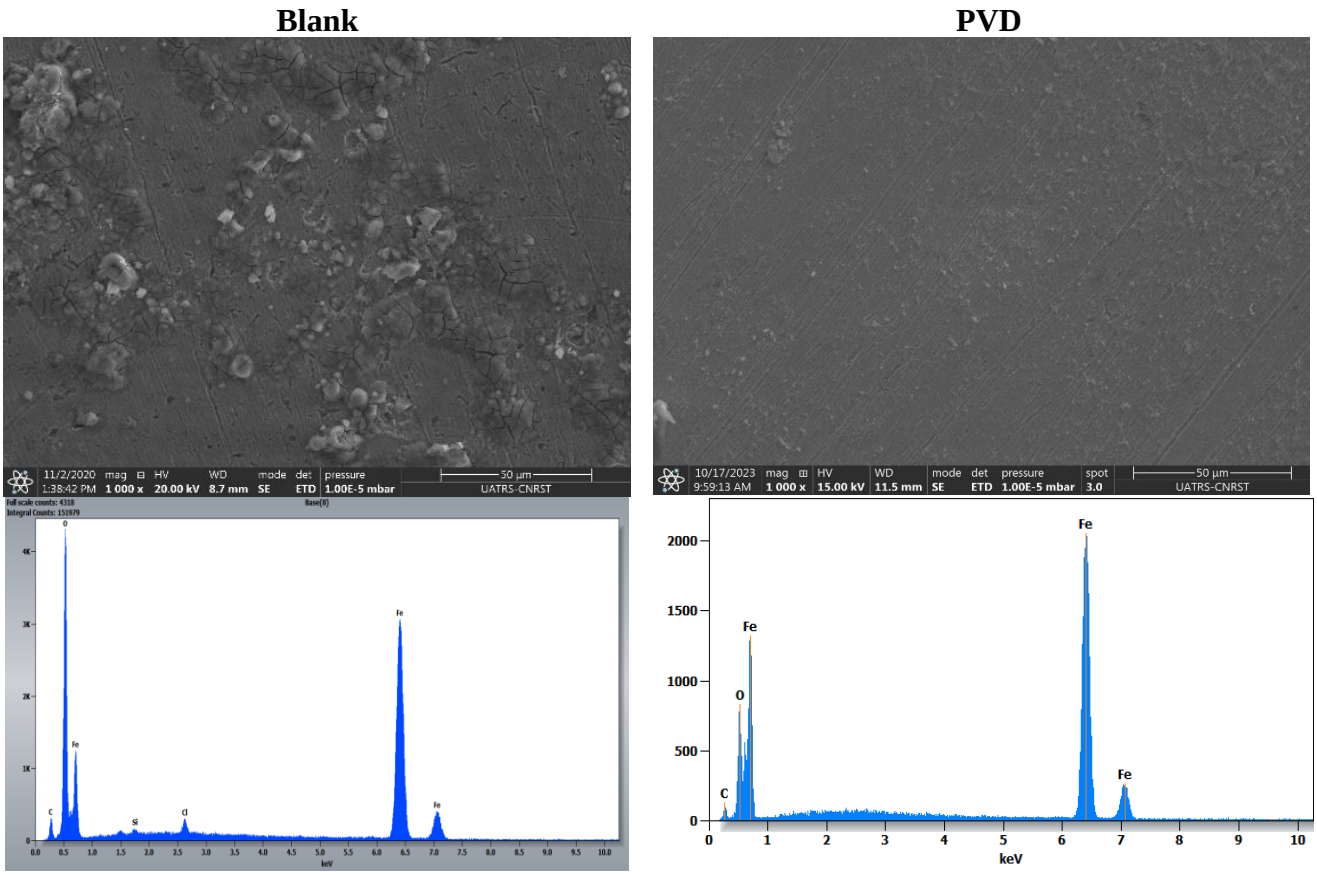

Figure 7: SEM/EDX images of mild steel substrates in the presence and absence of PVD oil essential.

Table 7: Percentage atomic contents of elements obtained from EDX spectra.

Eléments	% Mass of steel in Blank solution	% Mass of steel in blank solution with PVD
C	2.91	2.0
O	25.91	9.3
Si	0.35	--
Cl	1.04	--
Fe	69.79	88.7

4. Conclusions

The investigation of the PVD essential oil as a corrosion inhibitor of mild steel against the corrosion process in 1M HCl allowed the underneath results:

- PVD essential oil perform as a great anti-corrosion compound for the mild steel, outstandingly at inflated concentrations.
- PVD essential oil distinguished by a stronger inhibitory capability due to the structure's properties of the major components, even at high temperature.
- PDP curves unfold the mixed-type nature of PVD essential oil inhibitor.
- EIS measurements indicate that PVD essential oil controlled the activity of corrosion reaction and a great adsorption of the major components on the surface metal was took place.
- The physisorption of PVD essential oil components on the mild steel surface in 1M HCl adopts the Langmuir isotherm model.
- SEM and EDX surface analysis, reveal a significant improvement of the formed layer of PVD essential oil components on the metal surface morphology with reduction of the corrosive elements.

References

[1] S. Jyothi, Y. S. Rao, P. S. Ratnakumar. (2019). Natural product as corrosion inhibitors in various corrosive media: A review. Rasayan Journal of Chemistry. 12 (2): e537-e544.

[2] M. A. Dar. (2011). A review: plant extracts and oils as corrosion inhibitors in aggressive media. Industrial Lubrication and Tribology. 63 (4): e227-e233.

[3] A. Miralrio, A. E. Vázquez. (2020). Plant extracts as green corrosion inhibitors for different metal surfaces and corrosive media: a review. Processes. 8 (8): e942.

[4] B. U. Ugi, J. E. Boekom, P. B. Ashishie, P. U. Ubua. (2025). Scopolamine Alkaloid as Novel Green Inhibitor of Malleable Fe Corrosion Studied by EIS, DFT, PDP and SEM Techniques. Portugaliae Electrochimica Acta. 43 (1): e23-e35.

[5] M. Znini. (2019). Application of Essential Oils as green corrosion inhibitors for metals and alloys in different aggressive mediums. Arabian Journal of Medicinal and Aromatic Plants. 5 (3): e1-e34.

[6] D. Kesavan, M. Gopiraman, N. Sulochana. (2012). Green Inhibitors for Corrosion of Metals: A Review. Chemical Science Review and Letters. 1 (1): e1-e8.

[7] Huiles essentielles. Tome 2, Monographies relatives aux huiles essentielles, 6ème éd, AFNOR, Paris-La Défense, 2000.

[8] H. T. Zaher, M. A. Hefnawy, S. S. Medany, S. M. Kamel, S. A. Fadlallah. (2024). Synergetic effect of essential oils and calcium phosphate nanoparticles for enhancement the corrosion resistance of titanium dental implant. Scientific Reports. 14 (1): e1573.

[9] M. Taibi, A. Elbouzidi, D. Ou-Yahia, M. Dalli, R. Bellaouchi, A. Tikent, M. Roubi, N. Gseyra, A. Asehraou, C. Hano, M. Addi, B. El Guerrouj, K. Chaabane. (2023). Assessment of the Antioxidant and Antimicrobial Potential of *Ptychotis verticillata* Duby Essential Oil from Eastern Morocco: An In Vitro and In Silico Analysis. Antibiotics. 12 (4): e655.

[10] Z. Bensouda, E. Elassiri, M. Galai, M. Sfaira, A. Farah, M. E. Touhami. (2018). Corrosion inhibition of mild steel in 1 M HCl solution by Artemisia Abrotanum essential oil as an eco-friendly inhibitor. Journal of Materials and Environmental Science. 9 (1): e1851-e1865.

[11] K. Boumhara, M. Tabyaoui, C. Jama, F. Bentiss. (2015). Artemisia Mesatlantica essential oil as green inhibitor for carbon steel corrosion in 1 M HCl solution: Electrochemical and XPS investigations. Journal of Industrial and Engineering Chemistry. 29 (1): e146-e155.

[12] A. Batah, A. Anejjar, L. Bammou, M. Belkhaouda, R. Salghi, L. Bazzi. (2017). Carbon steel corrosion inhibition by rind and leaves extracts of grapefruit in 1.0 M hydrochloric acid. Journal of Materials. 8 (9): e3070-e3080.

[13] A. Salhi, A. Bouyanzer, I. Hamdani, A. Chetouani, B. Hammouti, M. Znini, L. Majidi, M. El Azzouzi. (2015). The use of essential oil and extract of Tetraclinis articulata as eco-friendly corrosion inhibitors of carbon steel in hydrochloric acid solution. Der Pharma Chemica. 7 (2): e138-e147.

[14] K. Benbrahim, B. El Mahi. (2017). Antibacterial activity and corrosion inhibition of mild steel in 1.0M hydrochloric acid solution by M. piperita and M. pulegium essential oils. Journal of Materials and Environmental Sciences. 8 (3): e972-e981.

[15] B. Zerga, M. Sfaira, Z. Rais, M. E. Touhami, M. Taleb, B. Hammouti, B. Imelouane, A. Elbachiri. (2009). Lavender oil as an ecofrindly inhibitor for mild steel in 1 M HCl. Matériaux & techniques. 97 (5): e297-e305.

[16] M. Znini, M. Bouklah, L. Majidi, S. Kharchouf, A. Aouniti, A. Bouyanzer, B. Hammouti, J. Costa, S. S. Al-Deyab. (2011). Chemical composition and inhibitory effect of Mentha spicata essential oil on the corrosion of steel in molar hydrochloric acid. International Journal of Electrochemical Science. 6 (3): e691-e704.

[17] Z. Bensouda, M. Driouch, R. A. Belakhmima, M. Sfaira, M. E. Touhami, A. Farah. (2018). Thymus sahraouian essential oil as corrosion eco-friendly inhibitor for mild steel in a molar hydrochloric acid solution. Portugaliae Electrochimica Acta. 36 (5): e339-e364.

[18] S. Andreani, M. Znini, J. Paolini, L. Majidi, B. Hammouti, J. Costa, A. Muselli. (2016). Study of Corrosion Inhibition for Mild Steel in Hydrochloric Acid Solution by Limbarda crithmoides (L.) Essential Oil of Corsica. J. Mater. Environ. Sci 7(1): e187-e195.

[19] K. Dahmani, M. Galai, M. Cherkaoui, A. El hasnaoui, A. El Hessni. (2017). Cinnamon essential oil as a novel eco-friendly corrosion inhibitor of copper in 0.5 M Sulfuric Acid medium. Journal of Materials and Environmental Sciences. 8(5): e1676-e1689.

[20] A. Salhi, A. Bouyanzer, I. El Mounsi, H. Bendaha, A. Chetouani, H. Amhamdi, A. Zarrouk, B. Hammouti, J. M. Desjobert, J. Costa. (2016). The inhibitive action of Pistacia lentiscus as a potential green corrosion inhibitor for mild steel in acidic medium. Moroccan Journal of Chemistry. 4 (4): e4.

[21] M. Znini, L. Majidi, A. Bouyanzer, J. Paolini, J. M. Desjobert, J. Costa, B. Hammouti. (2012). Oil of Salvia aucheri mesatlantica as a green inhibitor for the corrosion of steel in 0.5 M H_2SO_4. Arabian Journal of Chemistry (bank Sciences Direct).

[22] K. Mzioud, A. Habsaoui, M. Ouakki, M. Galai, S. El Fartah, M. Ebn Touhami. (2020). Inhibition of copper corrosion by the essential oil of Allium sativum in 0.5 M H_2SO_4 solutions. SN Applied Sciences. 2 (1): e1-e13.

[23] A. A. Hermas, M. S. Morad. (2008). A comparative study on the corrosion behaviour of 304 austenitic stainless steel in sulfamic and sulfuric acid solutions. Corrosion Science. 50 (9): e2710-e2717.

[24] M. Ouakki, M. Galai, M. Cherkaoui, E. H. Rifi, Z. Hatim. (2018). Inorganic compound (apatite doped by Mg and Na) as a corrosion inhibitor for mild steel in phosphoric acidic medium. Analytical and Bioanalytical Electrochemistry. 10 (7): e943-e960.

[25] A. Oubihi, M. Ouakki, A. Ech-chebab, E. H. E. Assiri, K. Tarfaoui, M. Galai, M. E. Touhami, M. Ouhssine, Z. Guessous. (2024). Corrosion inhibition in 1M HCl of mild steel with Thymus leptobotrys Murb essential oil (TLMEO): electrochemical measurements and Density Function Theory (DFT) and Molecular Dynamics (MD) simulations. Journal of Applied Electrochemistry. 1 (1): e1-e19.

[26] M. P. Desimone, G. Gordillo, S. N. Simison. (2011). The effect of temperature and concentration on the corrosion inhibition mechanism of an amphiphilic amido-amine in CO_2 saturated solution. Corrosion Science. 53 (12): e4033-e4043.

[27] H. E. Jamil, A. Shriri, R. Boulif, M. F. Montemor, M. G. S. Ferreira. (2005). Corrosion behavior of reinforcing steel exposed to an amino alcohol-based corrosion inhibitor. Cement and Concrete Composites. 27 (6): e671-e678.

[28] M. Beniken, R. Salim, E. Ech–chihbi, M. Sfaira, B. Hammouti, M. E. Touhami, M. Taleb. (2022). Adsorption behavior and corrosion inhibition mechanism of a polyacrylamide on C–steel in 0.5 M H_2SO_4: Electrochemical assessments and molecular dynamic simulation. Journal of Molecular Liquids. 348 (1): e118022.

[29] M. Yadav, L. Gope, N. Kumari, P. Yadav. (2016). Corrosion inhibition performance of pyranopyrazole derivatives for mild steel in HCl solution: gravimetric, electrochemical and DFT studies. Journal of Molecular Liquids. 216 (2): e78-e86.

[30] A. G. Allah, M. M. Hefny, S. A. Salih, M. S. El-Basiouny. (1989). Corrosion inhibition of zinc in HCl solution by several pyrazole derivatives. Corrosion. 45 (7): e574-e578.

[31] C. Verma, A. Alfantazi, M. A. Quraishi, K. Y. Rhee. (2023). Significance of Hammett and Taft substituent constants on bonding potential of organic corrosion inhibitors: Tailoring of reactivity and performance. Coordination Chemistry Reviews. 495 (1): e215385.

[32] A. Sehmi, H. B. Ouici, A. Guendouzi, M. Ferhat, O. Benali, F. Boudjellal. (2020). Corrosion inhibition of mild steel by newly synthesized pyrazole carboxamide derivatives in HCl acid medium: experimental and theoretical studies. Journal of the Electrochemical Society. 167 (15): e155508.

[33] A. Ramachandran, P. Anitha, S. Gnanavel, S. Angaiah. (2024). Development of 1-phenyl-3-(4-(pyridin-4-ylmethyl) phenyl) urea derivatives as robust corrosion inhibitors for mild steel in 1 M HCl environment: Insight from, molecular, experimental, and microscopic-scale modelling approaches. Journal of Environmental Chemical Engineering. 12 (1): e111648.

[34] L. C. Isaiah, N. B. Iroha. (2023). Evaluation of Mild Steel Corrosion Protection in 1 M HCl Solution by Vildagliptin: Experimental and Theoretical Studies. World Scientific News. 177 (1): e51-e67.

[35] M. Hrimla, L. Bahsis, A. Boutouil, M. R. Laamari, M. Julve, S. E. Stiriba. (2021). Corrosion inhibition performance of a structurally well-defined 1, 2, 3-triazole derivative on mild steel-hydrochloric acid interface. Journal of Molecular Structure. 1231 (1): e129895.

[36] K. E. Essien, A. O. Odiongenyi, E. J. BoEkom, O. E. Okon, I. O. Ekpenyong, N. O. Eddy, E. J. Abai. (2022). Corrosion Inhibition Potential of Two Isoxazole Derivatives: Experimental and Theoretical Analyses.

[37] M. Ouakki, M. Galai, M. Rbaa, A. S. Abousalem, B. Lakhrissi, E. H. Rifi, M. Cherkaoui. (2020). Investigation of imidazole derivatives as corrosion inhibitors for mild steel in sulfuric acidic environment: experimental and theoretical studies. Ionics. 26 (10): e5251-e5272.

[38] H. Wei, B. Heidarshenas, L. Zhou, G. Hussain, Q. Li, K. K. Ostrikov. (2020). Green inhibitors for steel corrosion in acidic environment: state of art. Materials Today Sustainability. 10 (2): e100044.

[39] X. Wang, J. Liu, Z. Zhang, Q. Xiang, J. Zhang, L. Chen, H. Xie. (2024). Mechanism for corrosion inhibition of pure iron in 1 M HCl by Rauiella Fujisana: Experimental, GCMS, DFT, VASP and solidliquid modeling studies. Industrial Crops and Products. 207 (1): e117692.

[40] Y. Boughoues, M. Benamira, L. Messaadia, N. Ribouh. (2020). Adsorption and corrosion inhibition performance of some environmental-friendly organic inhibitors for mild steel in HCl solution via experimental and theoretical study. Colloids and Surfaces A: Physicochemical and Engineering Aspects. 593 (1): e124610.

[41] I. Merimi, R. Touzani, A. Aouniti, A. Chetouani, B. Hammouti. (2020). Pyrazole derivatives efficient organic inhibitors for corrosion in aggressive media: A comprehensive review. International Journal of Corrosion and Scale Inhibition. 9 (4): e1237-e1260.

[42] L. M. Vračar, D. M. Dražić. (2002). Adsorption and corrosion inhibitive properties of some organic molecules on iron electrode in sulfuric acid. Corrosion Science. 44 (8): e1669-e1680.

[43] Y. El Ouadi, M. Lamsayah, H. Bendaif, F. Benhiba, R. Touzani, I. Warad, A. Zarrouk. (2021). Electrochemical and theoretical considerations for interfacial adsorption of novel long chain acid pyrazole for mild steel conservation in 1 M HCl medium. Chemical Data Collections. 31 (1): e100638.

[44] F. E. T. Heakal, S. A. Rizk, A. E. Elkholy. (2018). Characterization of newly synthesized pyrimidine derivatives for corrosion inhibition as inferred from computational chemical analysis. Journal of Molecular Structure. 1152 (1): e328-e336.

[45] M. Mehdipour, R. Naderi, B. P. Markhali. (2014). Electrochemical study of effect of the concentration of azole derivatives on corrosion behavior of stainless steel in H_2SO_4. Progress in Organic Coatings. 77 (11): e1761-e1767.

[46] S. El Arrouji, K. Karrouchi, A. Berisha, K. I. Alaoui, I. Warad, Z. Rais, S. Radi, M. Taleb, A. Zarrouk. (2020). New pyrazole derivatives as effective corrosion inhibitors on steel-electrolyte interface in 1 M HCl: Electrochemical, surface morphological (SEM) and computational analysis. Colloids and Surfaces A: Physicochemical and Engineering Aspects. 604 (1): e125325.

[47] A. Ousslim, A. Ouniti, K. Bekkouch, A. Elidrissi, B. Hammouti. (2009). Thermodynamic Study of Corrosion and Inhibitor Adsorption Processes on to C38 Steel/Piperazines/Phosphoric Acid Systems. Surface Review and Letters. 16 (4): e609-e615.

[48] S. H. Kumar, S. Karthikeyan. (2012). Inhibition of mild steel corrosion in hydrochloric acid solution by cloxacillin drug. Journal of Materials and Environmental Science. 3 (5): e925-e934.

[49] A. A. Al-Amiery, A. A. H. Kadhum, A. H. M. Alobaidy, A. B. Mohamad, P. S. Hoon. (2014). Novel corrosion inhibitor for mild steel in HCl. Materials. 7 (2): e662-e672.

[50] L. Herrag, A. Chetouani, S. Elkadiri, B. Hammouti, A. Aouniti. (2008). Pyrazole derivatives as corrosion inhibitors for steel in hydrochloric acid. Portugaliae Electrochimica Acta. 26 (2): e211-e220.

[51] K. Cherrak, O. M. A. Khamaysa, H. Bidi, M. El Massaoudi, I. A. Ali, S. Radi, Y. El Ouadi, F. El-Hajjaji, A. Zarrouk, A. Dafali. (2022). Performance evaluation of newly synthetized bi-pyrazole derivatives as corrosion inhibitors for mild steel in acid environment. Journal of Molecular Structure. 1261 (1): e132925.